

The optical and structural properties of polycrystalline Cu(In,Ga)(Se,S)₂ absorber thin films

F. B. Dejene

Received: 27 April 2011 / Accepted: 27 May 2011 / Published online: 17 June 2011
© Springer Science+Business Media, LLC 2011

Abstract The pentenary compound semiconductor Cu(In,Ga)(Se,S)₂ is one of the most attractive materials for high-efficiency solar cells due to its tunable band gap to match well the solar spectrum. In this study, semiconducting Cu(In,Ga)(Se,S)₂ thin films were prepared by a classical two-step growth process, which involves the selenization and/or sulfurization of In/Cu–Ga precursor. During the precursor formation step metallic In/Cu–Ga alloys were deposited onto the Mo-coated soda-lime glass substrates by DC magnetron sputter process. The respective precursors were subsequently reacted with H₂Se and/or H₂S gasses, at elevated temperatures. By optimizing the selenization parameters, such as the gas concentrations, reaction time, reaction temperature, and the flow of H₂Se and H₂S, high quality, single phase pentenary films were obtained. The gallium and sulfur diffusion behaviors were found to depend strongly on the selenization/sulfurization profile. The surface morphology, phase structure, and composition of the layers were analyzed by scanning electron microscope, atomic force microscopy, X-ray diffraction, and electron diffraction spectroscopy. Photoluminescence measurements were performed to examine the optical properties of the films.

Introduction

The CuInSe₂(CIS)-based ternary chalcopyrite semiconductor is the candidate with the best chances to compete with crystalline silicon. This promising material for the

fabrication of thin films solar cells have high-absorption coefficient ($\alpha = 10^5 \text{ cm}^{-1}$), suitable band gap ($E_g = 1.04 \text{ eV}$) and has long-term stability [1]. It has been shown that incorporating gallium into CIS to form Cu(In,Ga)Se₂ (CIGS) can increase the band gap up to 1.6 eV [2]. The material properties of CuInSe₂-based solar cells are critically influenced by their stoichiometric compositions [3] and defect chemistry, which in turn are strongly related to the films growth parameters. Over the past years various techniques were used to develop CIS and/or CIGS thin films and the conversion efficiencies of polycrystalline thin-films solar cell devices have steadily increased to values above 14 and 19.9% in the case of CuInSe₂/CdS/ZnO [4] and Cu(In,Ga)Se₂/CdS/ZnO [5], respectively. Therefore, a key issue to be addressed for further improvement of these solar cell devices is a correlation between the device characteristics of completed devices and the material properties (i.e., structural, optical, and electrical) of the CuInSe₂ and family absorber films. To achieve higher band gaps chalcopyrite thin films, which should lead to improve device performance, the use of sulfur and gallium to partially replace selenium and indium, respectively, together has been an interesting option. However, the atomic ratio for Ga in the >19% efficient CIGS solar cells is ~7%, which corresponds to a band gap of ~1.15 eV. CIGS solar cells with higher Ga amounts have lower efficiency. For example, CGS solar cells (which have a band gap of ~1.7 eV have a record efficiency of 9.5% for pure CGS and 10.2% for surface-modified CGS. A significant problem related to the two-step growth process is the reported segregation of Ga toward the Mo back contact, resulting in separated CuInSe₂ and CuGaSe₂ phases [6–11]. As a result, these layers are normally completely depleted of Ga in the near surface region of the absorber film, and the characteristics of

F. B. Dejene (✉)
Department of Physics, University of the Free State,
Private Bag X13, Phuthaditjhaba 9866, South Africa
e-mail: dejenebf@ufs.ac.za

completed solar cell devices are similar to those of devices produced from pure CuInSe₂ absorber layers. In this study, we present experimental evidence that the diffusion of gallium and sulfur toward the Mo back contact or toward the surface can be prevented in an optimized two-step growth process. The structural features of the homogeneous absorber layers are discussed and optical data are presented to illustrate the influence of the gallium and sulfur in cooperation on the optical band gap of the semiconductor thin films.

Experimental

Absorber formation

The CuIn_{0.75}Ga_{0.25} metallic precursors were deposited by DC (direct current) magnetron sputtering, in a system that accommodates three separate targets (Cu/Ga, In, and Mo). During absorber deposition the Mo-coated glass substrates, typically 1 cm² in size, were rotated continuously to promote uniformity and intermixing of Cu, In, and Ga. The Mo back contact was deposited at a working pressure and substrate temperature of around 10⁻³ mbar and 350 °C, respectively, and had a typical thickness of about 1 μm. The resulting Cu–In–Ga alloys were typically around 0.7 μm thick and were deposited with no intentional heating of the substrates at working pressures around 3 × 10⁻³ mbar. The typical chemical composition of the metallic precursors were 46.7 at.% Cu, 40.1 at.% In, and 13.2 at.% Ga. During the subsequent reaction process, the metallic precursors were first selenized in a horizontal reaction tube at reduced pressures in H₂Se diluted with Ar at temperatures 400 °C for periods of 30 min. These alloys were finally reacted to a H₂S/Ar atmosphere at a temperature of 550 °C for periods between 15 and 30 min to convert the films into single-phase, homogeneous Cu(In_{1-x}Ga_x)(Se_{1-y}S_y)₂ pentenary alloys. After the sulfurization step, the samples were allowed to cool to room temperature under Ar atmosphere.

Characterization

The morphological features of the two categories of films (sulfurized at 450 and 550 °C for 60 min) were examined by scanning electron microscopy (SEM) while the crystalline quality of the films was evaluated with normal incidence X-ray diffraction (XRD), using Cu Kα (0.154 07 nm) radiation. A Park Scientific Auto probe CP equipped with an AFM/LFM head was used for AFM measurements. The topography images were acquired in the constant force mode using the minimal force to keep the tip in contact with the sample. The bulk composition of the

sulfurized films was determined by energy dispersive X-ray spectroscopy (EDS). The in-depth concentration profiles of the samples were determined by X-ray photoemission spectroscopy (XPS), using a physics electronics (PHI) Quantum 2000 Scanning XPS system with Al Kα radiation at 20 W beam energy. The spot size was 100 μm, and the argon ion gun operated at 2 kV. The in-depth compositional analyses of the samples were studied with scanning X-ray photoelectron spectroscopy (SXPS) depth profiling.

Results

Structural features of the chalcopyrite thin films after sulfurization

In the first step of the reaction process, the metallic alloys were annealed in a diluted H₂Se/Ar atmosphere to convert the metallic coatings to composite coatings comprising a mixture of binary selenides and group I–III–VI ternary phases or a mixture of ternary phases, depending on the reaction conditions. In a standard procedure, the H₂Se gas concentration was fixed at specific levels, while the reaction temperature and time were used to control the degree of selenization (i.e., the volume fraction of binary phases converted into ternary phases). After the selenization step, the H₂Se gas was withdrawn from the horizontal reaction tube, and the selenized alloys were annealed in an atmosphere containing a mixture of H₂S and Ar under defined conditions. Figure 1a, b depicts the typical morphological features of the films after being selenized at 400 °C for 30 min, followed by a sulfurization step at (a) 450 °C and (b) about 500 °C. The gas concentration of H₂S in Ar was maintained at levels below 10 molar percent, while the sulfurization period was fixed at 30 min for this specific study. At sulfurization temperatures around 450 °C the films revealed the presence of rod-like crystallites superimposed on the small-grained background material (Fig. 1a, with less defined grain structure of typical sizes around 1 μm (inset Fig. 1b)) [12]. However, the high density of sub-micron grains corresponds to a significant increase in the grain boundary density in the thin film. This, in turn, may result in deterioration in the electrical behavior of the solar cell device. An increase in the sulfurization temperature to around 500 °C resulted in more observable structural changes due to the increased incorporation of S and produced films characterized by large conglomerates of larger crystals with regions of faceted grains mostly of 2–5 μm-size (inset Fig. 1b). The large crystallite and/or agglomerates in large areas of the film indicated that the recrystallization of the film was facilitated by a Cu-rich Cu(Se,S) or Cu_{2-x}Se phase, which is a quasi-liquid phase at temperatures around 500 °C [6]. This molten surface

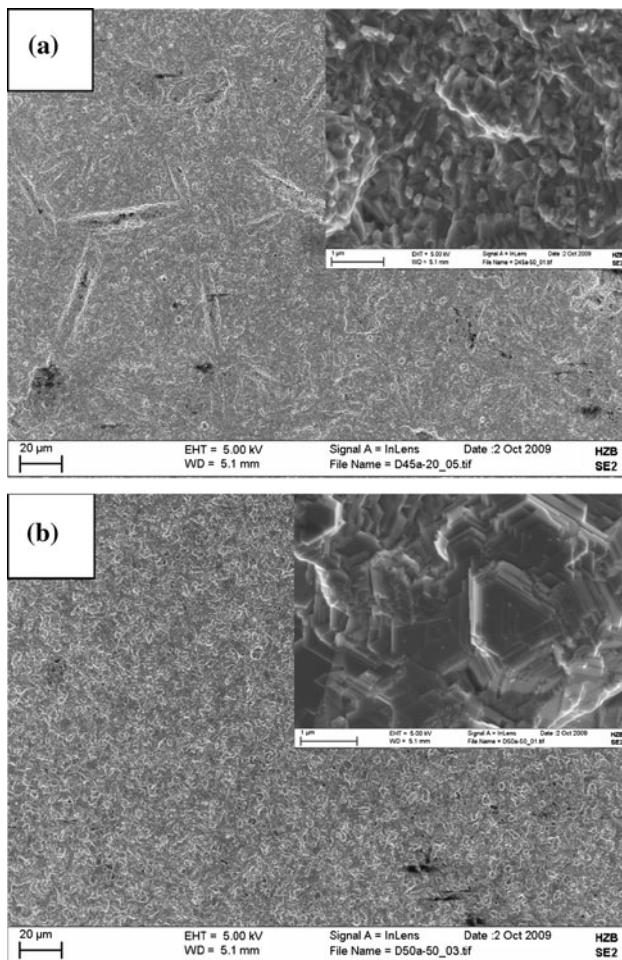


Fig. 1 SEM micrograph of the typical surface morphology of the reference $\text{Cu}(\text{In}_{1-x}\text{Ga}_x)(\text{Se}_{1-y}\text{S}_y)_2$ films after selenized at 400 °C for 30 min and sulfurized at temperatures around **a** 450 °C **b** 500 °C

phase is known to act as a ‘flux’ due to the high diffusion coefficients of the species involved in the growth process and has also been detected during the co-evaporation of $\text{Cu}(\text{In,Ga})(\text{Se,S})_2$ alloys [7, 13]. Reaction of the films to $\text{H}_2\text{S}/\text{Ar}$ at temperatures above 500 °C converted the composite alloy into a compact semiconductor alloy with superior structural features consisting of 2–5 μm grain structures. It is important to realize that the final surface morphology of a specific sample is significantly influenced by the overall bulk composition of the film. Therefore, for the purpose of comparison, the depicted films in Fig. 1 had comparable bulk compositional properties, with $\text{Ga}/(\text{In}+\text{Ga})$, $\text{S}/(\text{S}+\text{Se})$, and $\text{Cu}/(\text{In}+\text{Ga})$ atomic ratios close to 0.25, 0.35, and 0.9. The observed variation in structural features observed in Fig. 1a, b is therefore directly related to the fact that the sulfurization was done at different temperatures and not to variations in the bulk composition of the films. The composition of the specific film in Fig. 1a, b is given in Table 1. It is important to mention that the

morphological features of the precursor structures and $\text{Cu}(\text{In,Ga})(\text{Se,S})_2$ films, depicted in Fig. 1a, b, are representative and were confirmed by repetitive growth studies. Experimentally, it was found that the sulfurization period, reaction temperature, and position of the sulfur source with respect to the samples critically influenced the degree of gallium and sulfur incorporation into the CuInSe_2 absorber films. The morphology of the deposited films was also investigated by AFM. Figure 2 shows 2D and 3D AFM images of $\text{Cu}(\text{In}_{1-x}\text{Ga}_x)(\text{Se}_{1-y}\text{S}_y)_2$ thin films, which represent the surface morphology as well as microstructure, deposited by reaction of the films to $\text{H}_2\text{S}/\text{Ar}$ at temperatures between 450 and 500 °C. Figure 2a, c depicts the typical 2D morphological features of the films after being selenized at 400 °C for 30 min, followed by a sulfurization step at (a) 450 °C and (c) about 500 °C. The surface variations of images are displayed by brighter and darker regions representing higher and lower points, respectively. The figures indicate that all the films’ surfaces are composed of spherical particles but sulfurization at temperature above 500 °C produced relatively uniform morphology and dense films of high crystalline quality. The 3D AFM images of the surface of deposited thin films selenized at 400 °C for 30 min, followed by a sulfurization step at (b) 450 °C and (d) about 500 °C. Films deposited at 500 °C depict a uniform, compact grain growth while films deposited at 450 °C portray large, rough, non-uniform, and mostly uni-directional grain growth. This mono-orientation and random packing produces numerous voids which may induce a high resistivity, and is detrimental to property of the completed solar cell devices. In general, the increase in the sulfurization temperature leads to decrease in roughness and increase in uniformity in size distribution. This reveals that the surface roughness is related to the deposition conditions as well as selenization and sulfurization parameters. XRD studies also revealed a dramatic variation in the crystalline quality of the films. In the case where all the films were sulfurized at 450 °C for 60 min, under the conditions described above, XRD studies revealed the presence of a graded $\text{Cu}(\text{In}_{1-x}\text{Ga}_x)(\text{Se}_{1-y}\text{S}_y)_2$ structure (Fig. 3a). This phenomenon is represented by the asymmetric broadening of the characteristic [112], [220/204], and [312/116] diffraction peaks. In this regard, it is important to note that the position of the [112] diffraction peak close to 27.9° represents the lattice parameter of $\text{Cu}(\text{In,Ga})\text{Se}_2$, while the tail, due to increasing amounts of sulfur and gallium, extends all the way to the peak position of $\text{Cu}(\text{In,Ga})\text{S}_2$. It is therefore reasonable to assume that the surface of the absorber film contains more of $\text{Cu}(\text{In,Ga})\text{Se}_2$ and that the sulfur and gallium increases continuously toward the Mo back contact. These observations are in good agreement with other related studies and are attributed to the difference in the formation kinetics of

Fig. 2 Shows 2D and 3D AFM images of $\text{Cu}(\text{In}_{1-x}\text{Ga}_x)(\text{Se}_{1-y}\text{S}_y)_2$ thin films, which represent the surface morphology as well as microstructure, deposited by reaction of the films to $\text{H}_2\text{S}/\text{Ar}$ at temperatures between 450 (a, c) and 500 °C (b, d)

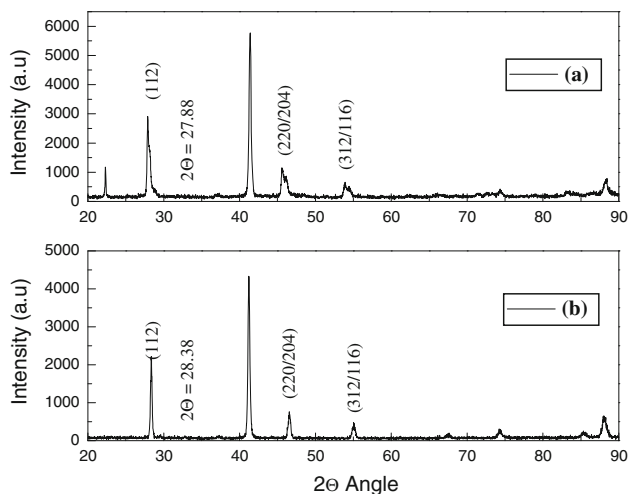
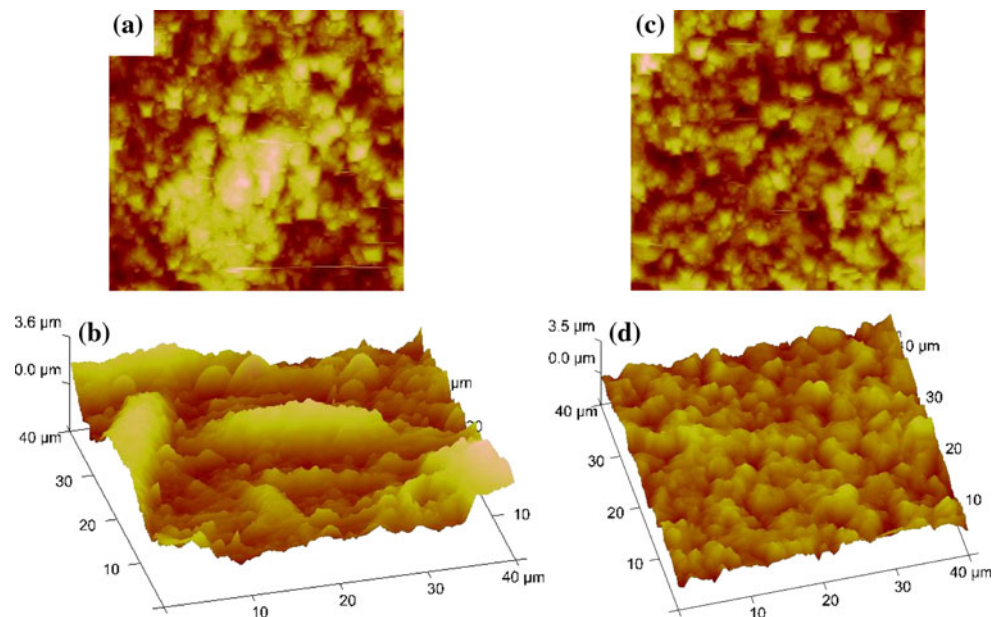


Fig. 3 XRD patterns of the $\text{Cu}(\text{In}_{1-x}\text{Ga}_x)(\text{Se}_{1-y}\text{S}_y)_2$ films after selenized at 400 °C for 30 min and sulfurized at temperatures around **a** 450 °C **b** 500 °C

the two ternary phases [8]. Figure 3b depicts a representative XRD pattern illustrating the crystalline quality of the films shown in Fig. 1b. It can be seen that a remarkable improvement in the crystalline quality was achieved when films were sulfurized at 550 °C for only 30 min. The extremely sharp, well-defined chalcopyrite peaks are indicative of the high crystalline quality of the pentenary alloys. The fact that the diffraction peaks are symmetric also indicates that the film is uniform and monophasic rather than compositionally graded, as observed in Fig. 3a. It is also important to note that the [112] peak position shifted toward a larger 2θ -value (from about 26.65° to 28.4°). This shift of the chalcopyrite reflection is in accordance with a decrease in the lattice parameter

associated with the homogeneous incorporation of gallium and sulfur into the pentenary $\text{Cu}(\text{In}_{1-x}\text{Ga}_x)(\text{Se}_{1-y}\text{S}_y)_2$ system. The degree of shift of the diffraction peak toward higher 2θ -values is exactly in accordance with Vegard's law [14], assuming single-phase material and a $\text{Ga}/(\text{Ga}+\text{In})$ and $\text{S}/(\text{Se}+\text{S})$ atomic ratio close to 0.25 and 0.35.

PL properties of the $\text{Cu}(\text{In}_{1-x}\text{Ga}_x)(\text{Se}_{1-y}\text{S}_y)_2$ thin films

The PL spectra for the $\text{Cu}(\text{In}_{1-x}\text{Ga}_x)(\text{Se}_{1-y}\text{S}_y)_2$ layers are presented in Fig. 4. These measurements were conducted at 77 K, and the broad bands suggest a donor–acceptor pair recombination, probably involving a copper vacancy (V_{Cu}) as an acceptor and indium or gallium on copper site (In_{Cu} , Ga_{Cu}) as donor, as the material is slightly In-rich. The PL response of a device quality slightly In+Ga-rich $\text{Cu}(\text{In}_{1-x}\text{Ga}_x)(\text{Se}_{1-y}\text{S}_y)_2$ is observed to be dominated by a broad donor–acceptor pair transition at approximately 1.0 and 1.25 eV. The expected increase in peak position in the PL responses, with uniform distribution of gallium and sulfur content, can clearly be seen. In order to estimate the band-gap energy, the binding energy of free excitons must be added to the energy position of the highest intensity line in the PL spectra, as indicated in Fig. 4. The values used for the binding energies for free excitons in CuGaSe_2 (14 meV), CuInSe_2 (7.5 meV), CuInS_2 (19 meV), and CuGaS_2 (29 meV) have been determined and reported elsewhere [15–17], and the binding energies of the $\text{Cu}(\text{In}_{1-x}\text{Ga}_x)(\text{Se}_{1-y}\text{S}_y)_2$ structures in our study were calculated using the linear dependence on x and y . These calculated band energies are estimated values, as they actually represent a value that is slightly lower than the true band-gap energy. All these results are summarized in Table 2.

Table 1 The elemental composition of the $\text{Cu}(\text{In}_{1-x}\text{Ga}_x)\text{Se}_2$ alloys in Fig. 1a, b

Sample no.	Elemental concentration (at.%)					Cu/III	Se+S/Me	Ga/Ga+In	S/Se+S
	Cu	In	Ga	Se	S				
A	20.87	18.74	5.98	33.55	8.39	0.934	0.920	0.242	0.20
B	20.15	17.46	5.82	29.01	15.66	0.912	1.030	0.250	0.35

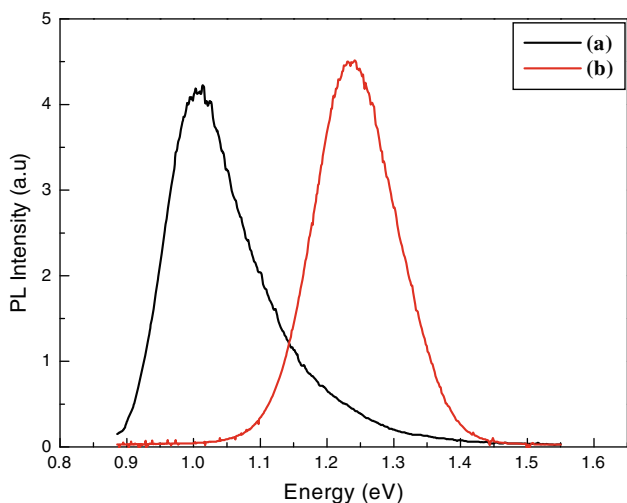


Fig. 4 PL spectra for $\text{Cu}(\text{In}_{1-x}\text{Ga}_x)(\text{Se}_{1-y}\text{S}_y)_2$ films after selenized at 400 °C for 30 min and sulfurized at temperatures around **a** 450 °C **b** 500 °C. Measurements were conducted at 77 K, using a 5 mW laser at an excitation wavelength of 514.5 nm. The increase of the broadband peak position with increasing gallium and sulfur content (increase in x and y) is observed

In-depth compositional uniformity of homogeneous $\text{Cu}(\text{In,Ga})(\text{Se,S})_2$ thin films

Figure 5 shows the in-depth compositional profiles of a typical homogeneous $\text{Cu}(\text{In}_{0.65}\text{Ga}_{0.35})(\text{Se,S})_2$ film with a $\text{Ga}/(\text{Ga}+\text{In})$ atomic ratio of approximately 0.35. The XPS depth profile results should be considered within the known limitation associated with depth profiling techniques using ion beam sputtering [18]. Against this background, it should be realized that the XPS results do not represent the exact compositional features of the compound, but are rather an indication of the distribution behavior of the elements in the bulk of the film. In this regard it is important to note that the concentration profiles of all the elements remained virtually constant in the region where the Mo signal was zero and decreased as soon as the Mo

signal became significant. An exceptionally higher content of gallium at the surface and at the bottom of the film, with a complementary low content value in indium peak, signifies that gallium was substituted for indium in the crystal structure. The homogeneous nature of the quaternary alloys prepared in this study partly agree with those chalcopyrite deposited by standard two-step processes, which exhibit an accumulation of Ga toward the Mo back contact [5–10]. The relatively constant $\text{Ga}/(\text{Ga}+\text{In})$ ratios in these films are in agreement with XRD results, indicating virtually no variation in d-spacing through the entire depth of the absorber films. The profile does not show any presence of oxygen signifying the absence of oxides of In, Ga, and Cu in the film. As seen in Fig. 5, no amount of silicon diffused into the film from the substrate.

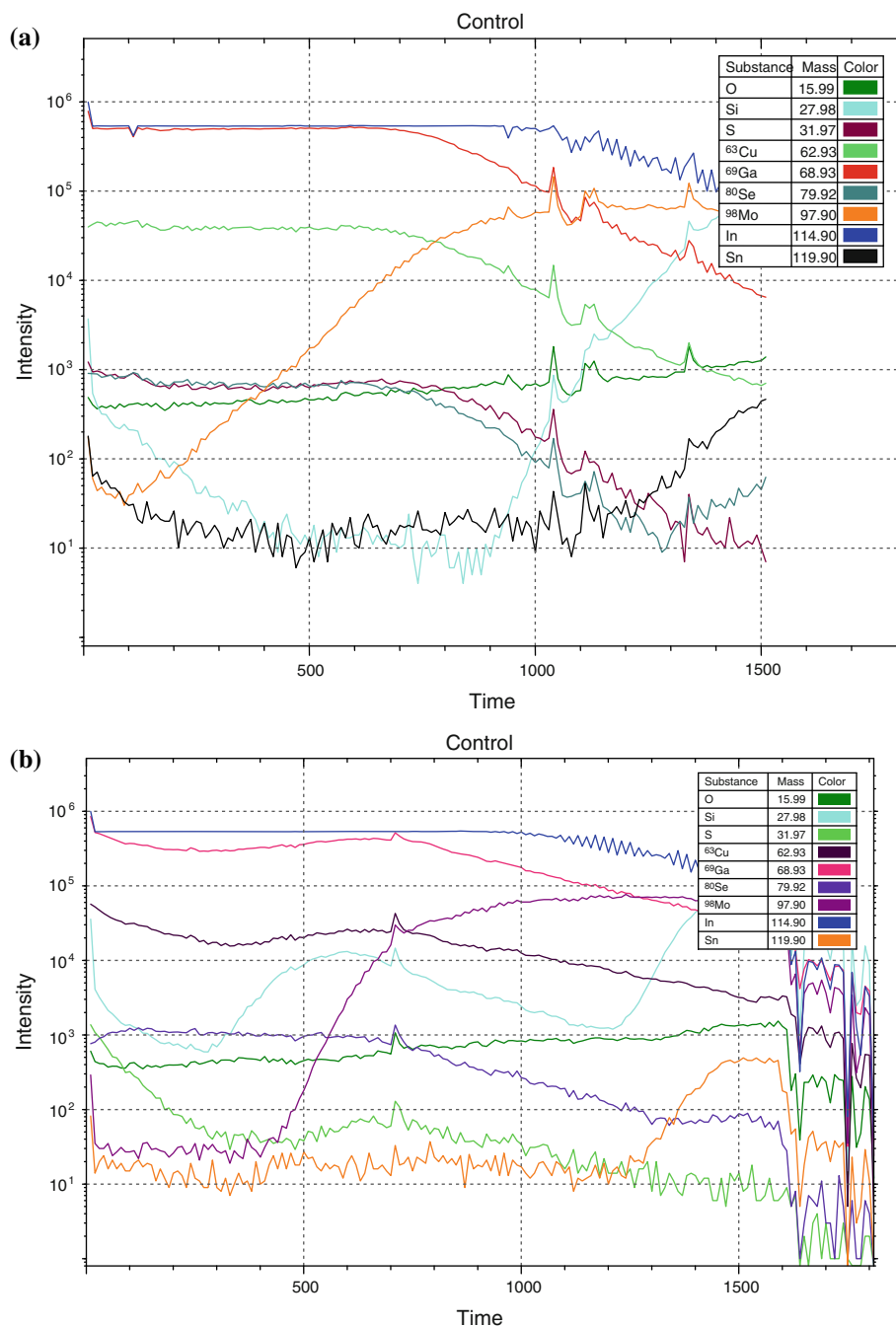
Conclusions

Systematic structural, morphological, compositional and optical measurements, such as PL spectroscopy dependence on the amount of gallium incorporation, were carried out on high-quality $\text{Cu}(\text{In}_{1-x}\text{Ga}_x)(\text{Se,S})_2$ polycrystalline thin films. It is demonstrated that the combination of controlled growth conditions delivers single-phase $\text{Cu}(\text{In,Ga})(\text{Se,S})_2$ films with a high degree of in-depth compositional uniformity. This was nicely highlighted by the XRD spectrum showing all $\text{Cu}(\text{In,Ga})(\text{Se,S})_2$ peaks, with shifts, indicating films with different gallium and sulfur incorporations. $\text{Cu}(\text{In,Ga})(\text{Se,S})_2$ peaks shifted to higher 2θ -values than $\text{Cu}(\text{In,Ga})\text{Se}_2$ due to a decrease in the lattice constant and increase in band gap of the materials. Optical studies also indicated an increase in band gap with increasing Ga and S content, confirming the homogeneous incorporation of Ga and S into the chalcopyrite lattice. These results were supported by SXPS measurements, revealing a uniform distribution of the elements through the entire depth of the alloy. The production of homogeneous $\text{Cu}(\text{In,Ga})(\text{Se,S})_2$

Table 2 Increase in calculated band-gap energy with increase in sulfur content for $\text{Cu}(\text{In}_{1-x}\text{Ga}_x)\text{Se}_2$ alloys

Structure	Calculated BE (meV)	Energy from PL (eV)	Estimated band gap (eV)
A = $\text{Cu}(\text{In}_{0.76}\text{Ga}_{0.24})(\text{Se}_{0.8}\text{S}_{0.2})_2$	57.29	1.00	1.06
B = $\text{Cu}(\text{In}_{0.75}\text{Ga}_{0.25})(\text{Se}_{0.65}\text{S}_{0.35})_2$	61.40	1.25	1.31

Fig. 5 XPS depth profile for $\text{Cu}(\text{In}_{1-x}\text{Ga}_x)(\text{Se}_{1-y}\text{S}_y)_2$ films after selenized at 400 °C for 30 min and sulfurized at temperatures around **a** 450 °C **b** 500 °C, clearly depict the distribution of the respective elements in the alloy



chalcopyrite thin films with tunable lattice parameters and band-gap values is an important prerequisite for fabricating high-efficiency solar cell devices. This gives clear evidence that $\text{Cu}(\text{In,Ga})(\text{Se,S})_2$ products will be important contenders on the PV power market.

Acknowledgements The author would like to thank Dr. Mutsumi Sugiyama and Prof. H. Nakanishi of the Tokyo University of Science Technology, Prof. S. F. Chichibu of the Tsukuba University for their help and fruitful discussions. He is also grateful to Prof. V. Albert of the University of Johannesburg for help with the experiments. X-ray photoelectron spectroscopy work by Martin van Staden and Werner Jordaan and AFM work by Prof. Tembela Hillie of CSIR microscopy

group are also gratefully acknowledged. The financial support of the National Research Foundation and University of Free State is acknowledged. The author, who is a Regular Associate of the Abdul Salam International Centre for Theoretical Physics (ICTP), Trieste, Italy, undertook part of this study with the support of ICTP.

References

1. Tuttle JR, Contreras MA, Ward JS, Gabor AM, Ramanathan KR, Tennant AL, Wang L, Keane J, Noufi R (1994) In: Proceedings of the IEEE First World conference on photovoltaic energy conversion, Waikoloa, pp 1942–1945

2. Marudachalam M, Birkmire RW, Hichiri H, Schultz JM, Swartzlander A, Al-Jassim MM (1997) *J Appl Phys* 82(2):2896
3. Alberts V, Swanepoel R, Witcomb MJ (1998) *J Mater Sci* 33:2919. doi:[10.1023/A:1004394328008](https://doi.org/10.1023/A:1004394328008)
4. Stolt L, Hedström J, Kessler J, Ruckl M, Velthaus K, Schock HW (1993) *Appl Phys Lett* 62(6):597
5. Contreras MA, Ramanathan K, AbuShama J, Hasoon F, Young DL, Egaas B, Noufi R (2008) *Prog Photovoltaics Res Appl* 13(3):209
6. Marudachalam M, Hichri H, Klenk R, Birkmire R, Shafarman W, Schultz J (1995) *Appl Phys Lett* 67:3978
7. Basol BM, Kapur VK, Halani A, Leidholm CR, Sharp J, Sites JR, Swartzlander A, Matson R, Ullal H (1996) *J Vac Sci Technol A* 14:2251
8. Marudachalam M, Birkmire RW, Hichri H, Schultz JM, Swartzlander A, Al-Jassim MM (1997) *J Appl Phys* 82:2896
9. Nakada T, Ohbo H, Wanatabe T, Nakazawa H, Matsui M, Kunioka A (1997) *Solar Energ Mat Sol C* 49:285
10. Nagoya Y, Kushiya K, Tachiyuki M, Yamase O (2001) *Sol Energ Mat Sol C* 67:247
11. Palm J, Probst V, Stetter W, Toelle R, Visbeck S, Calwer H, Niesen T, Vogt H, Hernandez O, Wendl M, Karg FH (2004) *Thin Solid Films* 451–452:544
12. Alberts V, dejene FB (2002) *J Phys D Appl Phys* 35:2021
13. Schön JH, Alberts V, Bucher E (1997) *Thin Solid Films* 301:115
14. Dejene FB, Alberts V (2005) *Appl Phys* 38(4):22
15. Chichibu S, Mizutani T, Murakami K, Shioda T, Kurafuji T, Hakanishi H, Fons PJ, Niki S, Yamada A (1998) *J Appl Phys* 83:3678
16. Meeder A, Fuertes Marron D, Chu V, Conde JP, Jager-Waldau A, Rumberg A, MCh Lux-Steiner (2002) *Thin Solid Films* 403–404:495
17. Tanakaa K, Uchikia H, Iidaa S, Terasakob T, Shirakatab S (2000) *Solid State Commun* 114:197
18. Galdikas A, Pranevicius L (2000) *Nucl Instrum Methods B* 164–165:868